# Modeling the barotropic response of the Mediterranean sea level to atmospheric pressure forcing

## D.A. Natsiopoulos⊠, G.S. Vergos, I.N. Tziavos

*Laboratory of Gravity Field Research and Applications, Department of Geodesy and Surveying, Aristotle University of Thessaloniki, Thessaloniki, GR-54124, Greece, +302310994366, dnatsio@topo.auth.gr*

## Abstract

An important characteristic of the Earth's atmosphere with direct impact on the marine environment and Earth's gravity field are the variations of the atmospheric pressure, as it often determines wind and weather patterns across the globe. Variations in atmospheric pressure and especially low atmospheric systems influence the values of radar altimeter sea level anomalies (SLA). This response of sea level is the Inverse Barometer (IB) correction given by altimeters within their geophysical data records. In this work, altimetric data sets from the satellite remote sensing mission of Jason-2 and their total inverse barometer corrections acquired by the on-board altimeters have been used for a period of fifty days. Atmospheric pressure data from the Live Access Server (LAS) of the National Oceanic and Atmospheric Administration (NOAA) are also implemented in order to study the variations in the sea level due to atmospheric pressure in Mediterranean Sea. Given the Jason-2 exact repeat period of ten days, the available data are used to examine the correlation between SLA variations and atmospheric forcing. Moreover, the IB correction (local and global) given by the altimeter is validated against the response of the sea level as well as its theoretical response. Additionally, a regional multiple regression analysis between sea level anomalies, the atmospheric pressure and wind speed components is carried out to model the barotropic response of the Mediterranean to atmospheric wind and pressure forcing. Finally, in order to investigate the IB effect in the frequency domain, a spectral transfer function has been computed through the Fourier transforms of sea level and pressure. At short scales of 10 days an agreement between the consecutive SLA records of the satellite is observed and the total IB correction given by the altimeter is closed to the expected one of the -1cm/hPa. In region with large discrepancies in air pressure the $b_1$ coefficient is close to -1 cm/bar while in areas with stable air pressure the other coefficients tend to have large values. The transfer function of IB presents large values and discrepancies when air pressure gets the minmax values and values close to zero when the air pressure is stable.

**Keywords**: SLA, barotropic response, regression analysis, atmospheric forcing

## 1. Introduction

Variations in atmospheric pressure and especially low atmospheric systems influence the sea level. In 1972, Wunsch examined the Bermuda sea level in relation to tides, weather and baroclinic fluctuations and found that continuum of sea level is dominated by pressure in an inverted barometer sense for periods shorter than a year while in 1973, Gill and Niller found an important response of sea level to changes in atmospheric pressure (Wunsch, 1972; Gill and Niiler, 1973). The expected response of sea level to atmospheric pressure change is one of major oceanic signals in tide gauge records. Similar works, have been also made in Mediterranean Sea where the response of the mean sea level to atmospheric pressure forcing is analyzed using altimetry data of mission of TOPEX/POSEIDON (Le Traon and Gauzelin , 1997). Within the above frame, the present work investigates the correlation between sea level variations and its response to atmospheric pressure change over short time scales for the Mediterranean Sea. Additionally, the validity of the classical expected response (- 1 cm/hPa) of sea level to atmospheric pressure change (Wunsch, 1972; Chelton and Davis, 1982; Chelton and Enfield, 1986) is examined through a multiple regression analysis (MGA) of sea level anomalies (SLAs), wind speed and atmospheric pressure data. Finally, the spectral transfer function between the SLAs and atmospheric pressure data is determined as well, to serve as an additional measure of the coherency between the two.

## 2. Sea level and atmospheric variations

In order to study the response of the sea level to atmospheric variations and forcing, single mission altimetry data from the Jason-2 satellite have been used. These refer to a period of ~2 months, between October-December 2013, along track pass 196, consisting of 6 repeat cycles (cycle 194 to 199). The specific time span was chosen because it was characterized by extremely low-pressure fields over the Mediterranean Sea and especially in the area of the Ionian and Adriatic Seas. Pass 196 consists of ~100-140 observations for each cycle, starting from northern Libya, passing east of Malta and crossing the Ionian and Adriatic Seas (Figure 2). Jason-2 data where acquired from the Radar Altimeter Database System of TU Delft (RADS 2012) which presents a collection of satellite altimetry data of past and current missions. The altimetric observations were available in the form of SLAs referenced to a "mean-sea-surface" that depends on user selection within the RADS system. Therefore, it was decided to refer the data to the EGM2008 geoid (Pavlis et al., 2012), keeping in mind that a zero-tide (ZT) geoid model is adopted to be in-line with the tide-conventions used in altimetric data processing. All geophysical and instrumental corrections have been applied, using the default models proposed by the RADS system. Those were a) ECMWF for the dry tropospheric correction, b) radiometer wet tropospheric correction for the wet tropospheric correction, c) the smoothed dual-frequency model for the ionospheric correction, d) tidal effects due to Solid Earth, Ocean, Load and Pole from the Solid Earth tide, GOT4.8 ocean tide, GOT4.8 load tide and pole tide models respectively, and e) the CLS non-parametric Sea State Bias (SSB) model for the SSB effect (Naeije et al., 2008). Atmospheric pressure and wind speed data for the period under study were available from the Live Access Server (LAS) of the National Oceanic and Atmospheric Administration (NOAA) provided at four times per day intervals in a grid format, the latter spans the entire Mediterranean Sea bounded between $30^\circ \leq \varphi \leq 50^\circ$ and $-10^\circ \leq \lambda \leq 40^\circ$ with a grid resolution of 5 arcmin. Given that the altimetric observations may contain voids in their records, either due to land intrusion and/or flagged entries in the geophysical data records, those have been removed so as to construct a complete and homogeneous database.

The first part of the performed work referred to the identification of sea level variations within the satellite repeat period, i.e., for periods as short as 10 days for Jason-2. This step aimed to identify whether the 10-day SLA variations follow a regular pattern, or some clear deviations can be identified. Later on the effort will be placed at contributing these variations to atmospheric forcing or other phenomena. In order to investigate such variations, a single pass was selected from the Jason-2 satellite based on the following criteria: a) the pass shall be long and span the entire basin in the north-south or south-north direction (ascending or descending pass respectively), b) there shall be no or little land intrusion from isles or islands in the SLA records, c) the data record shall be as consistent as possible throughout the satellite data record for the period of study, i.e., missing records and/or voids should be kept to a minimum (Vergos et al., 2012). Based on these criteria, it was decided that pass 196 for Jason-2 would be studied, being an ascending one, starting from northern Libya, passing East of Malta and crossing the Ionian and Adriatic Seas. The study period for the Jason-2 SLA data is between cycle 194 (15/10/2013) and cycle 199 (03/12/2013). Table 1 summarizes the statistics of the SLAs after the application of all geophysical corrections except for that of the global and local Inverse Barometer ones. An analytical description of the barometer correction is given in the following paragraph. From that table it is evident that the available Jason-2 SLAs present little variations in the first thirty days (cycles 194 to 196), with differences in the

**Table 1:** Statistics of Jason-2 SLAs per cycle [Unit: cm]

| cycle | date and time | values | min | max | mean | std |
|-------|---------------|--------|-----|-----|------|-----|
| 194 | 15/10/2013 09:45 | 88 | -7.43 | 8.60 | -0.13 | ±3.73 |
| 195 | 25/10/2013 07:44 | 107 | -13.45 | 9.72 | 1.94 | ±4.45 |
| 196 | 04/11/2013 05:42 | 149 | -7.71 | 9.77 | 2.08 | ±3.61 |
| 197 | 14/11/2013 03:41 | 131 | -10.76 | 26.03 | 12.21 | ±7.44 |
| 198 | 24/11/2013 01:39 | 134 | 3.10 | 31.42 | 18.11 | ±5.35 |
| 199 | 03/12/2013 23:38 | 146 | -22.48 | 8.86 | -9.36 | ±6.88 |

range and mean value up to 4 cm and 1.5 cm respectively. During November, these variations vary from 6 to 10 cm in the mean value while in the last 10 days there is as significant variation reaching 27 cm in terms of the mean value. Therefore it becomes apparent that a more detailed outlook per cycle is needed in order to detect SLA variations.

Figure 1 presents the Jason-2 SLAs for cycles 194-199, where the along-track differences between consecutive cycles can be investigated. It should be noted that as the satellite passes north from a latitude of 39.3º and up to a latitude of 42.3º, no SLA data are available due to land intrusion and errors in the Geophysical Data Records (GDRs) due to shallow bathymetry from the two peninsulas of the Puglia region (see also Figure 2). From Figure 1, it can be seen that the SLAs for cycles 194, 195 and 196 are in good agreement and they generally follow a pattern of oscillating lower and higher SLAs. Cycles 197 and 198 deviate considerably by as much as 25 cm from the former, indicating that some kind of forcing occurs in the SLA records. Note that while in the southern part of the region cycles 197 and 198 agree very well, this does not happen in the northern part, where cycle 197 is in (relative) agreement with cycles 194-196. The latter can lead to the conclusion that the source of SLA forcing present in the cycle 198 is absent in cycle 197.
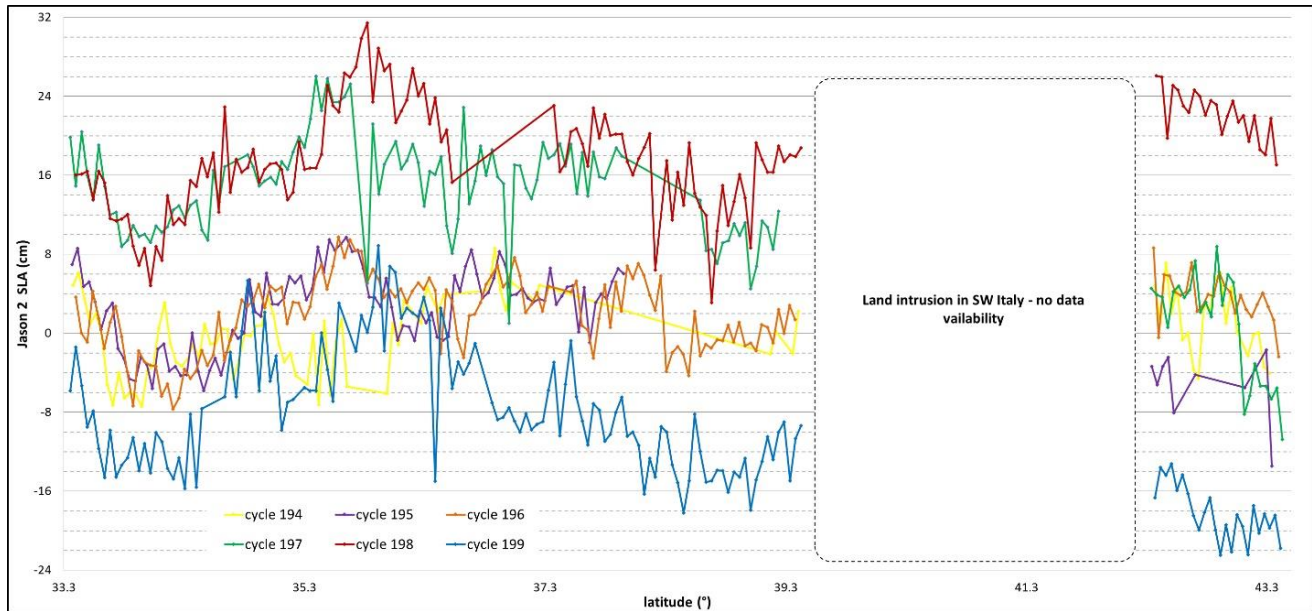


**Figure 1:** Jason-2 pass 196 SLAs for cycles 194 to 199.

In order to investigate the SLA variations within the above time period, the atmospheric pressure variations occurred have been examined as well. It is well-known that the sea level responds hydrostatically to changes in the atmospheric pressure, hence the corresponding corrections in the altimetric records, i.e., the IB correction, should be performed (Wunsch and Stammer, 1997). Of course the latter refers to studies where the contribution of atmospheric forcing needs to be removed, such as e.g., geoid and dynamic ocean topography related works. Within that frame, it was examined whether the total barometer correction given by the altimeter is close to the expected response of about *-1 cm/hPa* of sea level to atmospheric pressure change. As a result, the total IB correction and the sum of global and local IB correction given within the altimetric GDRs have been compared with the instantaneous IB effect on sea surface height. The latter has been computed from the surface atmospheric pressure data available $P^{atm}$ as:

$$IB^{est} = -9.948 \times (P^{atm} - \bar{P}) \tag{1}$$

where $IB^{est}$ is the estimated IB effect and $\bar{P}$ is the time varying mean of the global surface atmospheric pressure over the oceans, which was set equal to 1013.25 hPa. Eq. 1 contains two parameters that need further discussion. The adopted scale factor 9.948 cm/hPa is an empirical one estimated by Wunsch (1972) and corresponds to the IB response at mid latitudes. Note that this mode of calculation follows the AVISO 2008 algorithms for the construction of corrected sea surface heights from the original altimetric observations. It will be a matter of discussion at a later section whether this rather simple fashion of computing the sea level response to atmospheric forcing is appropriate and whether the scale factor applies to the area and time period under study or a more regional index should be employed (Ponte 1993, 1997). Moreover, we have set the time varying mean atmospheric pressure equal to a constant value, i.e., 1013.25 hPa so that we would not have to compute a time-varying average. For the current experiment, where we need to address whether the sea level variations in the area and period under study can be attributed to atmospheric and wind forcing, this assumption does not introduce biases. On the other hand, if the employed Jason-2 SLAs would be studied in combination with Topex/Poseidon data, then the time varying mean value of 1010.9 hPa adopted in the latter and the consequent difference with the currently adopted value should be considered (see also the discussion in the Jason1/2 handbook (AVISO, 2011)).

Within Eq. (1), $P^{atm}$ will come from the available surface atmospheric pressure data for the period under study. In Figure 2 atmospheric pressure values at sea level, for the period and area under study, are depicted. The atmospheric pressure data used are values from LAS of NOAA given four times per day on a 5 arcmin grid, spanning the entire Mediterranean Sea and bounded between $30^{o} \leq \varphi \leq 50^{o}$ and $-10^{o} \leq \lambda \leq 40^{o}$. For each cycle two sets of data are plotted depending on the time of the satellite, except for the cycle 199 where only air pressure at 00:00 is depicted because the satellite passed the region a few minutes earlier. Air pressure values at sea level vary from 1000 to 1040 hPa within this 50-day period. For most dates, air pressure is close to 1010-1020 hPa. On December 4th the highest values are observed (1030-1040 hPa) while the smallest ones are observed ten days earlier when it is near 1000 hPa. Figure 3 and Table 2 present the statistics and the variation of the available from the GDRs and computed with Eq. 1 IB corrections. Comparing Figure 1 and Figure 2, the inverse relation between SLAs and IB effects is clearly visible. When calm atmospheric pressure conditions prevail over cycles 194, 195 and 196 (~1020 hPa) the IB correction is moderate in the along-track direction of the pass and has a variation of 3-4 cm only. A slight exception is the north part of the track for cycle 196 on November 4, where an atmospheric low is formed and the pressure drops by ~10 hPa, with a consequent large increase in the IB correction of ~10 cm (see also Figure 1 the deviation of cycle 196 in the northern part compared to cycles 194 and 195). This situation changes drastically for cycles 197 and 198, where a lower pressure field in the southern part of the pass prevails with the atmospheric pressure dropping by 10 hPa and the IB having a range of 10 cm. Cycle 198 is dominated by the atmospheric low over central-eastern Mediterranean with the pressure dropping from 1010 hPa to ~1003 hPa), the latter presenting a 20 hPa pressure change compared to the quite field of cycles 194 and 195. The IB correction has again a large range of 12 cm being also 25 cm higher than the minimum observed for cycle 195. For cycle 199 the area is dominated by high-pressure being around 1018 hPa for the southern part and 1026 hPa for the northern one.

As far as the IB corrections themselves are concerned, Table 2 presents a) the total IB as derived by the MOG2D (2D gravity waves model) of Lynch and Gray (1979) representing the high frequency atmospheric forced variability, b) the sum of local high-frequency and global low-frequency IB correction as calculated from ECMWF 6-hr pressure data and given in the altimetric records and c) the IB correction as calculated by Eq. 1 using the atmospheric pressure values from NOAA's LAS (see Figure 2). As pointed out by Carrère and Lyard (2003) the classic IB correction applied in the altimetric data, models only the static part of the ocean response to atmospheric forcing and completely neglects wind effects, which prevail in the high- and low-latitude, and more energetic, areas. Note however that the area under study is not at high latitudes so it remains to be seen whether the simple IB correction computed with Eq. 1 is sufficient to reduce the SLA variance. Small differences (2 – 5 cm) are observed between the correction while the IB correction given by equation (1) is closest to the sum of local and global values. In some cycles the global value of IB was not available and as result the sum is equal to the local correction. As a result, local IB correction given by the altimeter represent very good the local pressure

field and the correction is close to correction calculated (AVISO, 2011). Finally, the barometer correction given by the altimeter is close to the expected response (-1 cm/hPa) of sea level to atmospheric pressure change (Wunsch, 1972; Gill and Niiler, 1973; Chelton and Enfield, 1986]. This is logical as the region of the pass is not very big and the period is less than a week (Ponte et al., 1991; Ponte, 1993).

**Table 2:** Statistics of IB corrections per cycle. [Unit cm]

| 194 | min | max | mean | std | 195 | min | max | mean | std |
|------|------|------|------|------|------|------|------|------|------|
| total | -8.81 | -5.63 | -7.70 | ±1.09 | total | -11.28 | -8.31 | -9.50 | ±0.67 |
| local+global | -9.81 | -7.14 | -8.71 | ±0.94 | local+global | -12.01 | 2.17 | -10.73 | ±0.44 |
| IB calculated | -6.67 | -5.17 | -6.18 | ±0.62 | IB calculated | -8.65 | -6.67 | -7.50 | ±0.53 |
| 196 | min | max | mean | std | 197 | min | max | mean | std |
| total | -11.12 | -3.15 | -8.22 | ±2.46 | total | -10.37 | 0.00 | -2.04 | ±3.16 |
| local+global | -8.51 | 1.47 | -5.27 | ±3.02 | local+global | -2.73 | 4.10 | 2.17 | ±2.14 |
| IB calculated | -6.67 | 3.28 | -3.85 | ±3.09 | IB calculated | -2.69 | 1.79 | 0.69 | ±1.36 |
| 198 | min | max | mean | std | 199 | min | max | mean | std |
| total | 1.93 | 13.25 | 6.24 | ±3.23 | total | -12.12 | -6.36 | -8.07 | ±1.95 |
| local+global | 3.50 | 10.66 | 7.34 | ±2.27 | local+global | -12.26 | -4.26 | -6.64 | ±2.71 |
| IB calculated | 3.78 | 9.75 | 7.31 | ±2.10 | IB calculated | -12.63 | -4.68 | -7.12 | ±2.87 |

## 3. Multiple regression analysis and spectral transfer function

A regional multiple regression analysis between sea level anomalies, the atmospheric pressure and wind speed components is carried out to model the barotropic response of the Mediterranean to atmospheric wind and pressure forcing. As with the air pressure data, wind speed data components have been collected from the LAS of NOAA. The wind speed used are wind speed vectors (m/sec) at 10 meters above ground on the same hour and date with air pressure values provided by LAS of NOAA given four times per day in a 0.05º grid format spanning the entire Mediterranean Sea bounded between $30º \leq \varphi \leq 50º$ and $-10º \leq \lambda \leq 40º$. For each cycle two sets of data are plotted depending on the time of the pass, except for the cycles 196 and 199. For the cycle 196 wind speed data is a mean field estimated between the 00:00 and and the 06:00 field. For the cycle 199 only wind speed at 00:00 is depicted because the satellite passed the region a few minutes earlier. Two different approaches for the linear regression between sea level wind speed and atmospheric pressure have been used. The first one with three regression coefficients nad the second one with five regression coefficients In the 3-coefficients case, they represent atmospheric pressure and two wind speed components, one in the West-East and another in the North-South direction for the point under consideration (Tsimplis and Vlahakis, 1994). In the 5-coefficients case there are two additional wind speed components for the preceding and following points (Wunsch, 1991; Fu and Pihos, 1994). The simple linear regression models when estimating 3 and 5 coefficients are outlined as :

$$sla = b_1 p + b_2 v_x + b_3 v_y \tag{2}$$

$$sla = b_1 p + b_2 v_{x-2} + b_3 v_{x+2} + b_4 v_{y-2} + b_5 v_{y+2} \tag{3}$$

where $p$ is atmospheric pressure in hPa, $v_x$ and $v_y$ are wind speed components in the two directions. Table 3 and Table 4 summarize the estimated coefficients for both cases investigated.
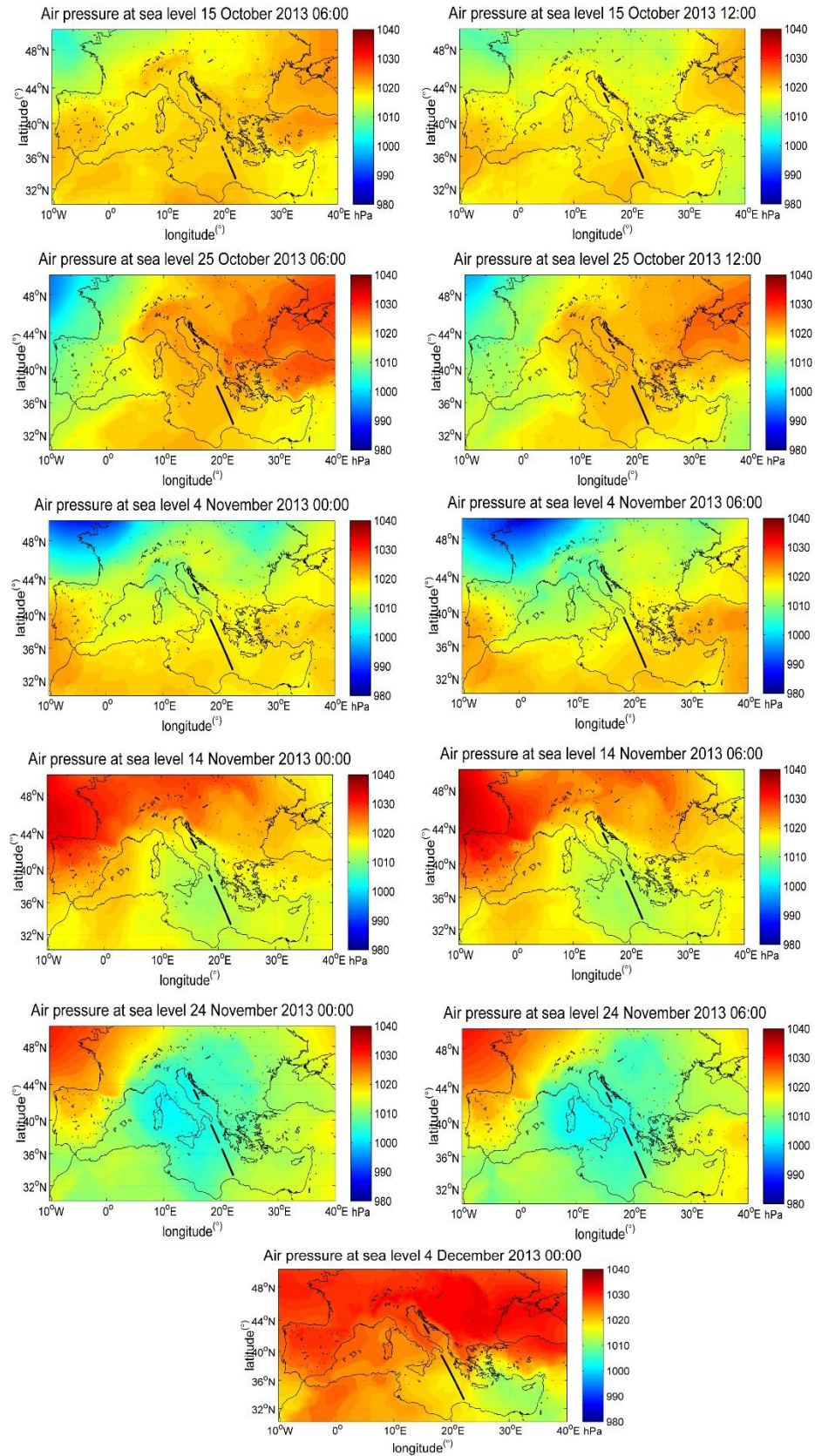
**Figure 2:** Atmospheric pressure at sea level over the Mediterranean from the period under study.
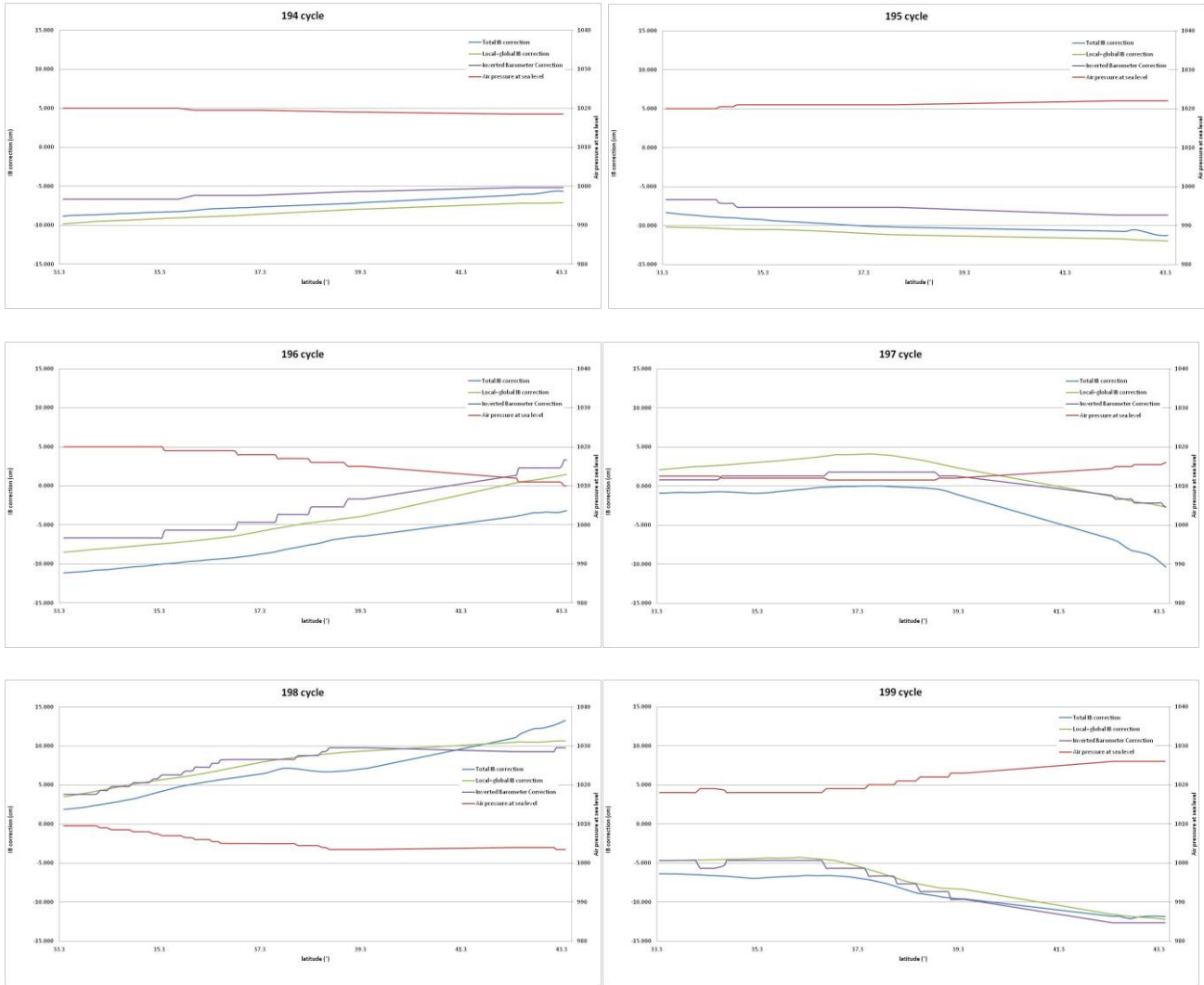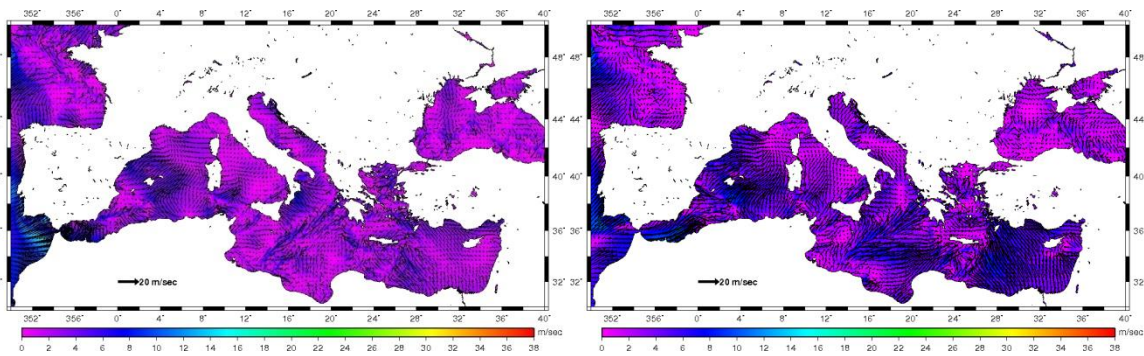
**Figure 3:** Air Pressure (hPa) at sea level and various IB corrections (cm) for all cycles
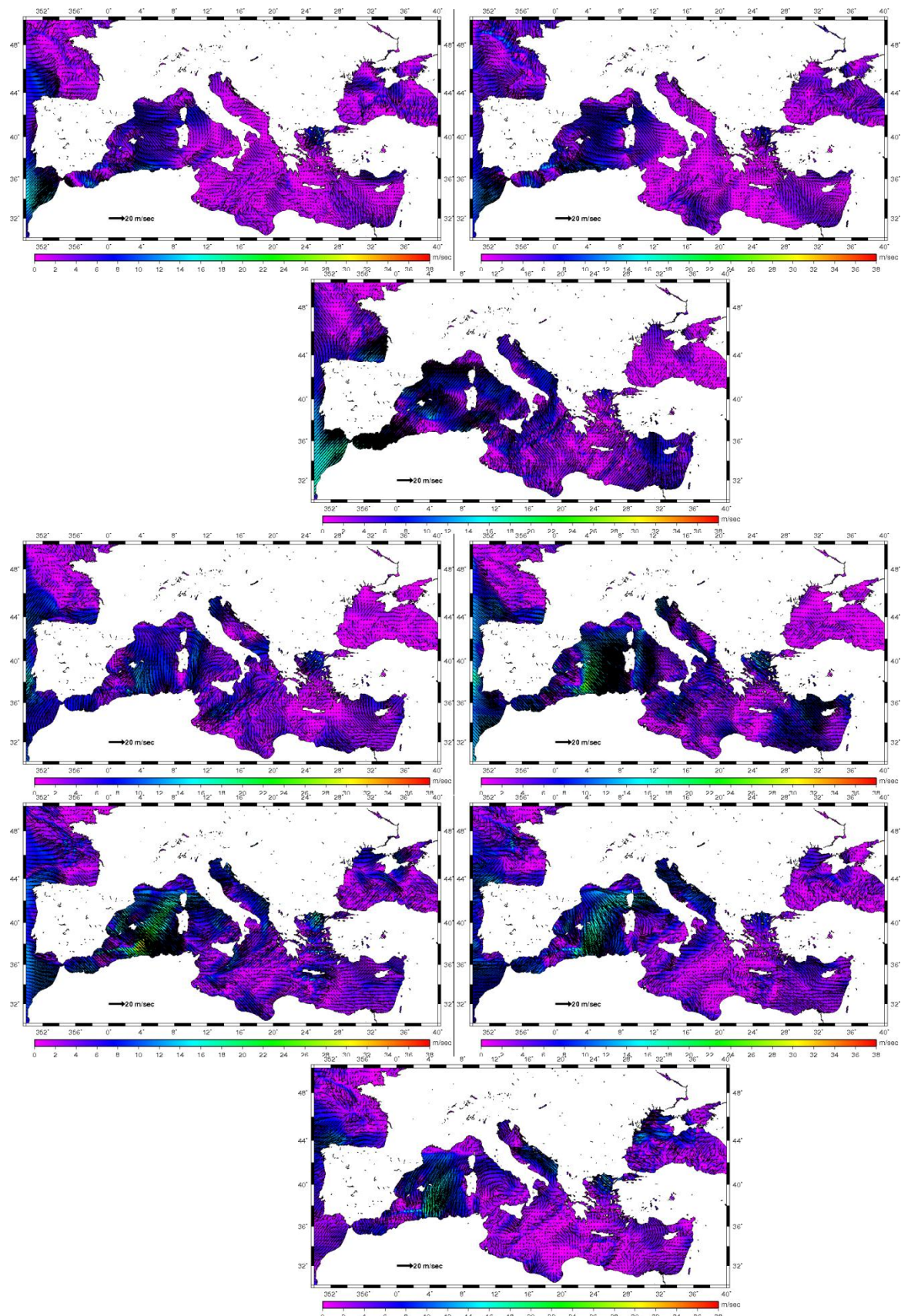
**Figure 4:** Wind speed vector (m/sec) at 10 meters above ground. The fields correspond to the dates outlined in Figure 3.

**Table 3:** Coefficients for 3-coefficients case

| cycle | $b_1$ (cm/hPa) | $b_2$ (m/s) | $b_3$ (m/s) |
|---|---|---|---|
| 194 | -0.108 ± 0.131 | 0.265± 0.541 | 1.645 ±1.202 |
| 195 | 0.041 ± 0.153 | 2.341 ± 0.660 | -0.541 ± 0.42 |
| 196 | 0.139 ± 0.126 | 0.110 ± 0.306 | 0.117 ± 0.241 |
| 197 | 1.166 ± 0.082 | 1.149 ± 0.445 | 1.789 ± 0.272 |
| 198 | 1.970 ± 0.421 | -0.032 ± 0.582 | -0.246 ± 0.72 |
| 199 | -1.122 ± 0.145 | -1.104 ± 0.260 | 1.540 ± 0.342 |

**Table 4:** Coefficients for 5-coefficients case

| cycle | $b_1$ (cm/hPa) | $b_2$ (m/s) | $b_3$ (m/s) | $b_4$ (m/s) | $b_5$ (m/s) |
|---|---|---|---|---|---|
| 194 | -0.163±0.150 | -0.667±1.048 | 0.933±1.931 | 1.817±2.429 | 0.182±2.309 |
| 195 | 0.088±0.115 | -3.624±1.374 | 3.772±1.442 | 6.491±1.806 | -6.647±1.875 |
| 196 | 0.088±0.234 | -2.741±0.579 | 2.416±1.321 | 1.327±1.147 | -0.857±1.478 |
| 197 | 1.189±0.086 | 1.231±0.735 | 0.162±0.714 | 0.434±1.566 | 1.318±1.655 |
| 198 | 1.530±0.511 | -2.280±1.357 | 1.972±1.239 | 0.675±0.984 | -0.216±1.013 |
| 199 | -1.071±0.130 | -2.289±0.843 | 1.178±0.870 | 0.553±0.893 | 1.248±0.840 |

In the 3-coefficients case, the coefficient for the atmospheric pressure in cycle 199 gets closer to the -1 cm/hPa while cycles 195 and 196 present small positive values. Values similar to the ones mentioned above have been found (Wunsch, 1991). However, cycles 197 and 198 present positive values close to 1 cm/hPa. Values similar to these have not been found in similar approaches and this is a fact to be investigated. In the case of 5-coefficients, $b_2$ to $b_5$ for the wind stress tend to have comparable magnitudes and opposite signs (Fu and Pihos, 1994). For the cycle 197 magnitude of the coefficients get smaller values signalling the pass of the atmospheric low in the area. For the cycles 197, 198 and 199 the high value of $b_1$ dictates that the SLA is mainly atmosphere-drive. Contrary to that for cycle 194, 195 and 196 is very low signalling that the SLA variation is due to other phenomena (salinity, temperature, steric effects, etc.). Finally, in order to investigate the IB effect in the frequency domain, a spectral transfer function has been computed through the Fourier transforms of sea level and pressure (Fu and Pihos, 1994). The spectral transfer function $F(\omega)$, has been computed with as:

$$F(\omega) = H(\omega)/P(\omega) \tag{4}$$

where $\omega$ is frequency and $H$ and $P$ are the Fourier transforms of sea level and pressure respectively.

In cycles where air pressure gets the min-max values (cycles 198-199) the transfer function present large discrepancies and large values while in cycles where air pressure values were stable the transfer function gets values close to zero. The coherency between SLA and air-pressure for Cycles 197, 198 and 199 is close to 50% and reduces to 10-20% for cycles 195, 196 and 197. Amplitudes like the ones mentioned above are found and in similar studies (Fu and Pihos, 1994), so it can be concluded that that coherency between sea level and pressure is strong and IB effect is detected. Given that the maximum span of the investigated track is ~1000 km the normalized frequency in Figures 5-10 corresponds to [cy/km]. Especially over cycles 197, 198 and 199, the correlation between atmospheric pressure and sea level can be seen up to ~200-250 km, where the admittance function has normalized amplitudes between 0.5 and 0.2 After these distances, and for the semi-enclosed Mediterranean Sea, atmospheric forcing to sea level variations is negligible.
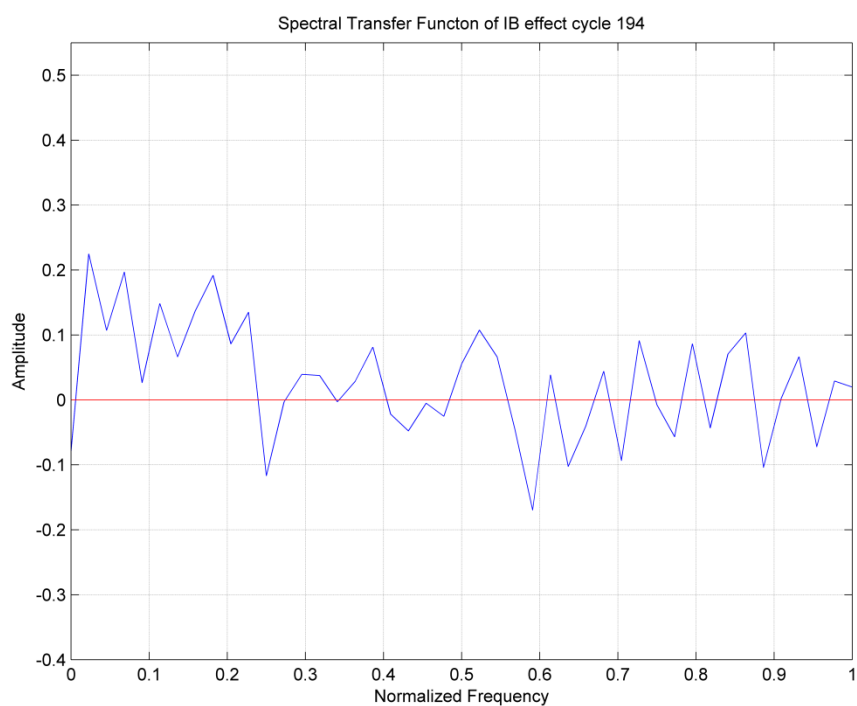
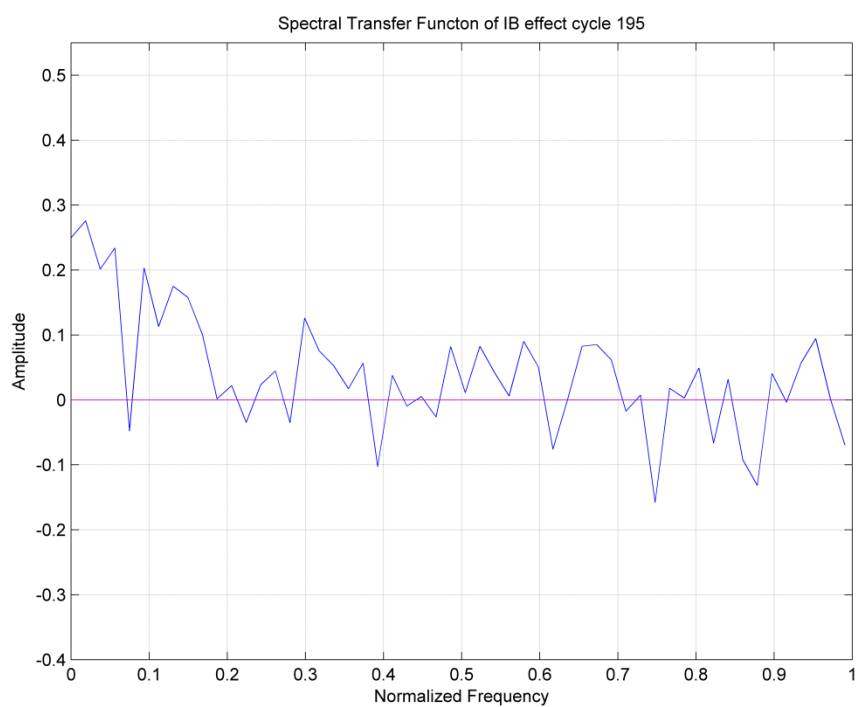**Figure 5:** Spectral Transfer Function of IB effect cycle 194



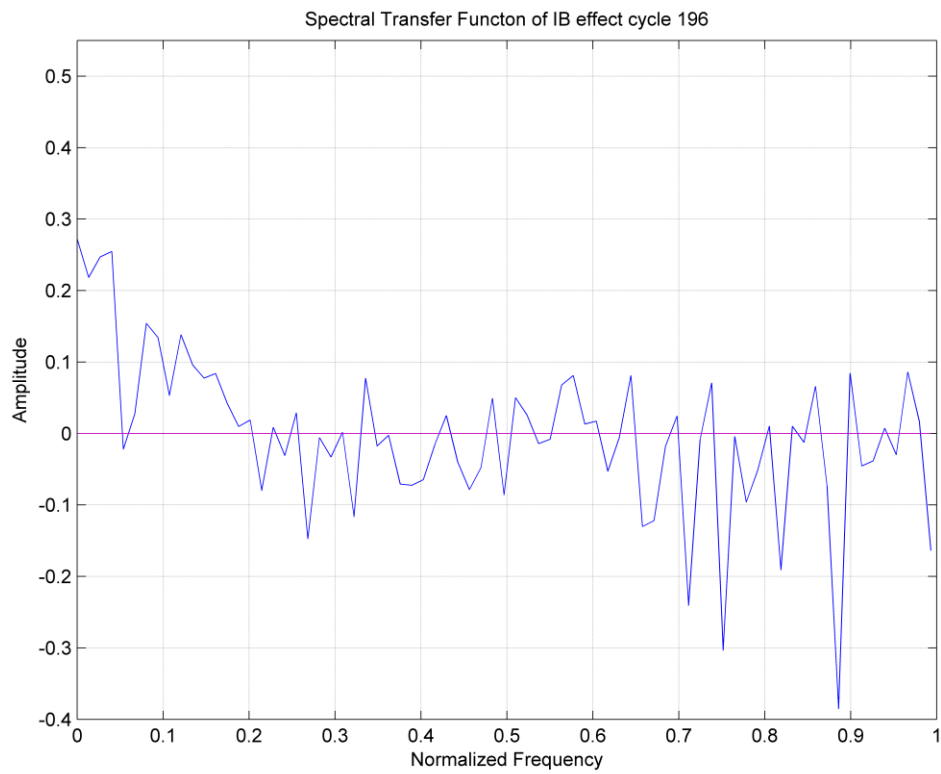**Figure 6:** Spectral Transfer Function of IB effect cycle 195

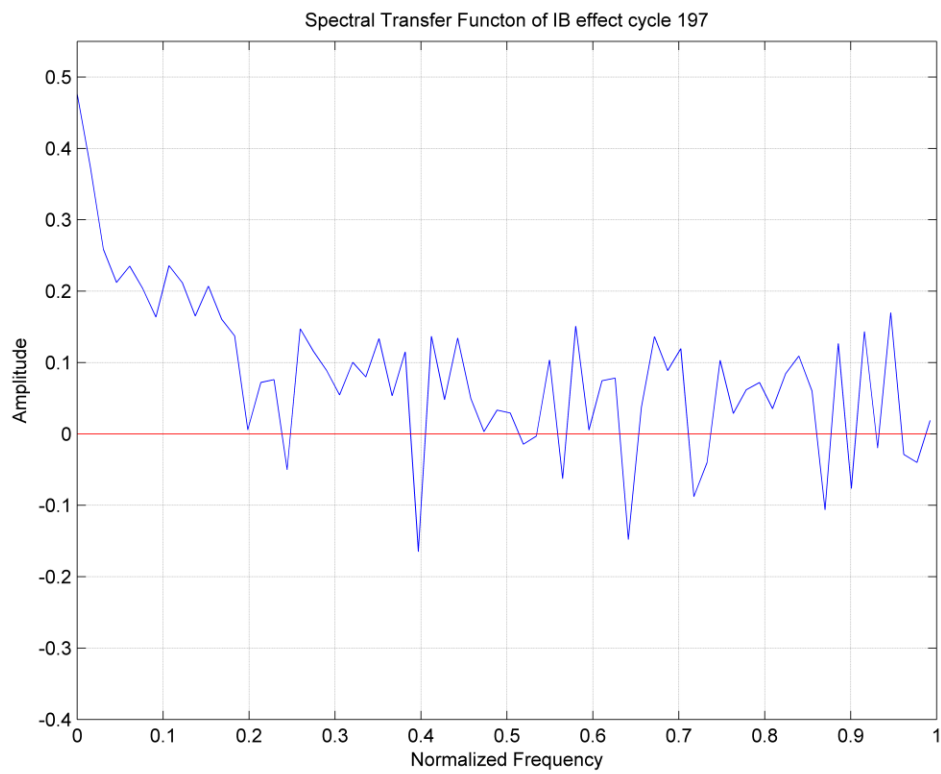**Figure 7:** Spectral Transfer Function of IB effect cycle 196.



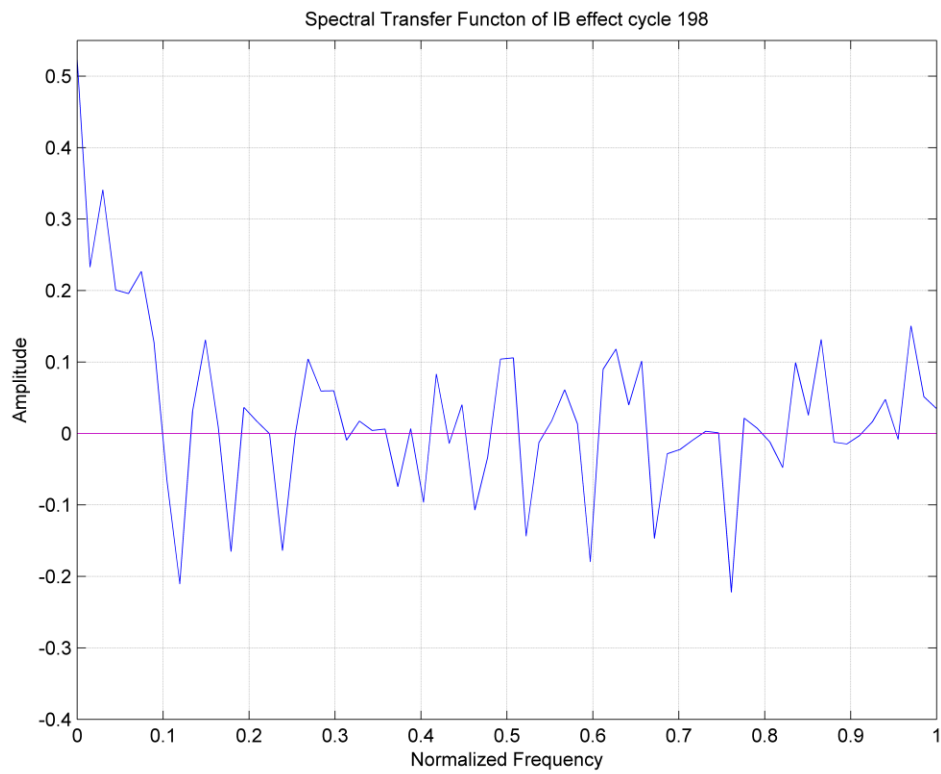**Figure 8:** Spectral Transfer Function of IB effect cycle 197.

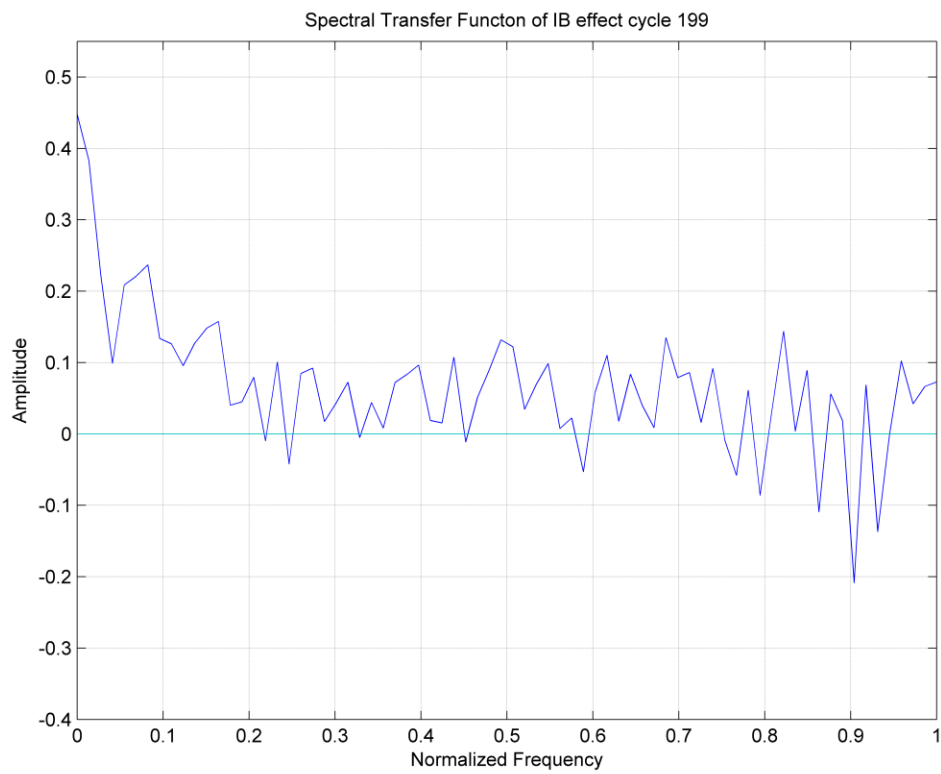**Figure 9:** Spectral Transfer Function of IB effect cycle 198.



**Figure 10:** Spectral Transfer Function of IB effect cycle 199.

## Conclusions

In this study along-track records of the SLA raw data have been used both to study variations in the sea level due to atmospheric pressure in Mediterranean Sea in short scales and examine if the barometer correction given by the altimeter is close to the response of sea level to atmospheric pressure. At short scales of 10 days an agreement between the consecutive SLA records of the satellite is observed. Differences between them, from cycle to cycle, can be attributed to extreme high and low pressure fields or high wind speeds. Generally, the total IB correction given by the altimeter is closed to the expected one of the -1cm/hPa and all types of IB corrections present similar values. Moreover, a regional multiple regression analysis between sea level anomalies, the atmospheric pressure and wind speed components is carried out to model the barotropic response of the Mediterranean to atmospheric wind and pressure forcing. Through multiple regional analysis, it is obvious that in region with large discrepancies in air pressure the $b_1$ coefficient is close to -1 cm/bar. The effect of wind forcing is obvious in areas with stable air pressure as the other coefficients tend to have large values. Finally, in order to investigate the IB effect in the frequency domain, a spectral transfer function has been computed through the Fourier transforms of sea level and pressure. The transfer function of IB presents large values and discrepancies when air pressure gets the minmax values and values close to zero when the air pressure is stable. There is large coherency between the SLA and atmospheric pressure when there is an atmospheric low, whereas it reduces to 10-20% when the SLA variation is not related to atmospheric forcing.

## References

AVISO (2011) IGDR and GDR Jason Products, SMM-MU-M5-OP-13184-CN, v. 4.1.

Carrère L and Lyard F (2003) Modeling the barotropic response of the global ocean to atmospheric wind and pressure forcing - comparisons with observations. Geophysical Res Lett 30(6): 1275. doi: 10:1029/2002GL016473.

Chelton DB and RE Davis (1982) Monthly mean sea-level variability along the west coast of North America. J Phys Oceanogr 12: 757-784.

Chelton DB and DB Enfield (1986) Ocean signals in tide gauge records. J Geophys Res 91(B9): 9081–9098. doi:10.1029/JB091iB09p09081.

Fu L and Pihos G (1994) Determining the response of sea level to atmospheric pressure forcing using TOPEX/POSEIDON data. J Geophys Res 99(C12): 24633–24642. doi: 10.1029/94JC01647.

Gill  AE and Niiler PP (1973) The theory of the seasonal variability in the ocean. Deep Sea Res Oceanogr Abstr 20: 141 – 177.

Le Traon Pierre-Yves and Gauzelin P (1997) Response of the Mediterranean mean sea level to atmospheric pressure forcing. J Geophys Res 102(C1): 973-984.

Lynch DR and Gray WG (1979) A wave equation model for finite element tidal computations. Computers and Fluids 7: 207-228.

Naeije M, Scharroo R, Doornbos E, Schrama E. (2008) Global Altimetry Sea Level Service: GLASS. NIVR/SRON GO project: GO 52320 DEO.

Pavlis NK, SA Holmes, SC Kenyon, and JK Factor (2012) The development and evaluation of the Earth Gravitational Model 2008 (EGM2008). J Geophys Res 117(B4): B04406. http://dx.doi.org/10.1029/2011JB008916.

Ponte RM, DA Salstein and RD Rosen (1991) Sea level response to pressure forcing in a barotropic numerical model. J Phys Oceanogr 21: 1043-1057.

Ponte RM (1993) Variability in a homogeneous global ocean forced by barometric pressure. Dyn Atm Ocean 18(3-4): 209-234. doi: 10.1016/0377-0265(93)90010-5.

Ponter RM (1997) Nonequilibrium Response of the Global Ocean to the 5-Day Rossby–Haurwitz Wave in Atmospheric Surface Pressure. J Phys Ocean 27(10): 2158-2168.

Ponte RM and Gaspar P (1999) Regional analysis of the inverted barometer effect over the global ocean using Topex/Poseidon data and model results. J Geophys Res 104 (C7): 15587-15601. doi: 10.1029/1999JC900113.

RADS-DEOS (2011) Available from: http://rads.tudelft.nl (Radar Altimeter Database System). Accessed January 2011.

Tsimplis MN and GN Vlahakis (1994) Meteorological forcing and sea level variability in the Aegean Sea. J Geophys Res 99(C5): 9879–9890. doi:10.1029/94JC00479.

Vergos GS, Natsiopoulos DA, Tziavos IN (2012) Sea level anomaly and dynamic ocean topography analytical covariance functions in the Mediterranean Sea from ENVISAT data. Presented at the European Space Agency "20 Years of progress in radar altimetry" Conference, September 24th-29th, Venice, Italy.

Wunsch C (1972) Bermuda sea level in relation to tides, weather, and baroclinic fluctuations. Rev Geophys 10(1): 1-49. doi: 10.1029/RG010i001p00001.

Wunsch, C (1991) Large-scale response of the ocean to atmospheric forcing at low frequencies. J Geophys Res 96(C8): 15083-15092.

Wunsch and Stammer (1997) Atmospheric loading and the oceanic inverted barometer effect. Rev Geophys 35(1): 79-107. doi: 10.1029/96RG03037.